Asymmetric Catalysis

Axially Chiral Imidodiphosphoric Acid Catalyst for Asymmetric Sulfoxidation Reaction: Insights on Asymmetric Induction**

*Garima Jindal and Raghavan B. Sunoj**

Abstract: *Insights into chiral induction for an asymmetric sulfoxidation reaction involving a single oxygen atom transfer are gained through analyzing the stereocontrolling transition states. The fitting of the substrate into the chiral cavity of a new class of imidodiphosphoric Brønsted acids, as well as weak C−H···π and C−H···O noncovalent interactions, are identified as responsible for the observed chiral induction.*

The chirality of drug molecules has long been known to play a vital role in their biological activities.[1] While impressive methodologies in asymmetric synthesis are now available,[2] the progress on catalytic methods for imparting chirality to heteroatoms, such as a sulfur atom, remain rather slow. Ever since the use of omeprazole and esomeprazole, two of the best selling sulphur-containing chiral prescription drugs,[3] the synthesis of chiral sulfur compounds has received more attention.[4] Similarly, chemical applications of sulfoxides as chiral auxiliaries[5] and its connection with human neuro-degeneration has helped garner attention for chiral sulfoxides.[6]

The conversion of an achiral sulfide into a chiral sulfoxide can be accomplished by asymmetric oxidation using enzymes[7] or transition-metal catalysis.[4] It is encouraging to note that environmentally benign H_2O_2 is now widely employed as an oxygen source in sulfoxidation reactions, and is in line with the contemporary quest for atom-economic and greener catalytic methods.[4f] In recent times, asymmetric organocatalytic methods to access sulfoxides have evolved as an effective strategy.[8] The emergence of axially chiral binol-based Brønsted acids and a whole gamut of its applications is particularly noteworthy.[9] A select set of highly successful examples of this family of binol variants (**I** and **II**) is shown in Figure 1.

In general, these axially chiral Brønsted acids have been demonstrated to be capable of imparting exceptionally high enantioselectivities in asymmetric aldol, Mannich, Friedel–Crafts, Diels–Alder, imine hydrogenation, and Tsuji–Trost allylation reactions.[9] The larger substituents at the 3,3′-
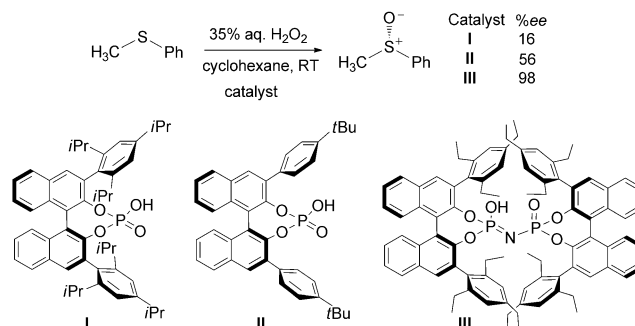
[*] G. Jindal, Prof. R. B. Sunoj
    Department of Chemistry, Indian Institute of Technology Bombay
    Powai, Mumbai 400076 (India)
    E-mail: sunoj@chem.iitb.ac.in
    Homepage: http://www.chem.iitb.ac.in/~sunoj

Figure 1. Commonly used binol phosphoric acids (**I** and **II**) and confined imidodiphosphoric acids (**III**).[10]
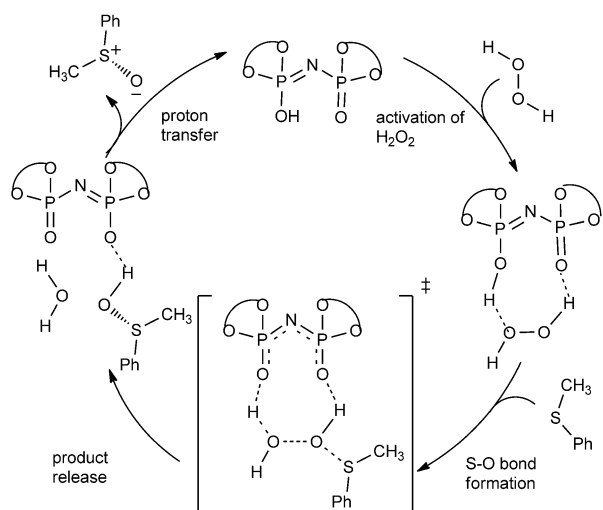
positions of the binol framework, such as that in 2,4,6-triisopropylphenyl, are known to be vital for obtaining a high degree of stereoselectivity.[9j–n] However, the efficiency of catalysts **I** and **II** in sulfoxidation was reported to be unexpectedly low.[10] Interestingly, axially chiral imidodiphosphoric acids (**III**) are found to be excellent catalysts for asymmetric sulfoxidation and reactions such as spiroacetalization and acetalization.[10,11] For instance, the group of List has noted high *ee* values in the sulfoxidation of thioanisole using aqueous H_2O_2 (Figure 1).[10] A few conspicuous questions at this stage are: a) What is the mode of catalysis, for example, activation of the reactant(s), as well as how is chirality transfer accomplished? and b) What is the origin of high efficacy of **III** where **I** fails to induce enantioselectivity in sulfoxidation? While there have been mechanistic studies on the issue of chiral induction in binol catalysis by the groups of Goodman, Himo, Terada, and others,[9j–n] the transition-state (TS) models for this new and promising axially chiral imidodiphosphoric acids have not yet been reported. The proposed mode of catalysis within a confined active site, akin to that in enzymatic reactions, is still an emerging concept in organocatalysis.[12] Furthermore, insights into chirality transfer in single-atom transfers, such as in stereoselective protonation or oxygen transfer (as in the present case), is inherently important. A suitable TS model will help bridge the gap between chemical and enzymatic catalysis. To exploit the catalytic potential and to broaden the scope of this novel form of catalysis, adequate mechanistic insights as well as the stereocontrolling elements responsible for chiral induction are highly desirable.

As part of our continued interest in understanding the origin of chiral induction, we herein present the first DFT-(M06-2X) TS models, involving chiral imidodiphosphoric acids, for the title reaction.[13] The discussion employs the Gibbs free energies obtained at the M06-2X/6-31G** level of

Scheme 1. General mechanism for the oxidation of sulfides into sulfoxides.

Figure 2. Optimized geometries of stereocontrolling transition states for **I**. The relative Gibbs free energies (kcal mol^{-1}) are provided within parentheses. All distances are in Å.

theory.[14] Geometry optimizations have also been carried out at the B3LYP-D3 and B3LYP levels of theory to compare the extent and significance of dispersive interactions.[14e] The mechanism of oxygen transfer can be envisaged as shown in Scheme 1, and consists of the electrophilic activation of H$_2$O$_2$ by the chiral Brønsted acid, the formation of the S−O bond between the activated H$_2$O$_2$ and thioanisole, the cleavage of the peroxide linkage and an accompanying proton transfer from the phosphoric acid leading to the formation of water, and proton transfer from the protonated sulfoxide back to the phosphate oxygen atom to regenerate the catalyst.

Within a chiral environment, such as in the presence of an axially chiral binol phosphoric acid, the interaction of the activated H$_2$O$_2$ with the incoming thioanisole can exhibit distinct preferences for certain prochiral modes of approaches. The approach of the oxygen atom to both the *re* and *si* faces of thioanisole is examined. Different conformers for the stereocontrolling S−O bond formation TSs are considered as well, to identify the most preferred mode.[15]

The role of the chiral Brønsted acid catalyst should be regarded as twofold: a) to drive the reaction through a catalytic pathway, and b) to provide a chiral environment for the chirality transfer. The relative energy of the TS for the S−O bond formation is found to be as high as 50 kcal mol^{-1} in the uncatalyzed route.[16] The O−O bond cleavage, transfer of a proton to H$_2$O$_2$, and the formation of the S−O bond are found to be a concerted process.[17a] The binding energy of H$_2$O$_2$ to **III** is found to be −9.8 kcal mol^{-1}, whereas that of thioanisole is only −1.2 kcal mol^{-1}.[17b] This difference shows that H$_2$O$_2$ is activated prior to the reaction. The relative energy of the corresponding TS in the imidodiphosphoric acid catalyzed (**III**) pathway with respect to separated H$_2$O$_2$, substrate, and catalyst is only 7.8 kcal mol^{-1}. The phosphoric acid renders electrophilic activation of H$_2$O$_2$ through a fairly strong hydrogen-bonding interaction and leads to significant lowering of the TS energy.

First, the factors contributing to the stereoinduction by **I**, bearing 2,4,6-triisopropylphenyl substituents at the 3,3′-posi-
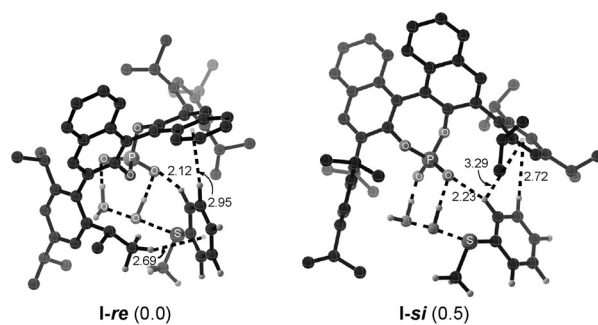
tions of the binol phosphoric acid, are analyzed. We have located the stereocontrolling TSs for the sulfoxidation of thioanisole using **I**.[18] The optimized geometries of the two most preferred TSs are given in Figure 2. In the lower-energy TS **I**-*re*, two interesting C−H···π interactions are identified; one between the phenyl ring of thioanisole and the isopropyl group (2.69 Å), and one between the phenyl ring of thioanisole and the naphthyl π face (2.95 Å). Another weak C−H···O interaction (2.12 Å) is also identified. Similar weak interactions are also evident in the higher energy TS **I**-*si* wherein the oxygen atom approaches the Si face of thioanisole. A common geometric feature in these diastereomeric TSs is that the methyl group of the thioanisole does not interact with the catalyst. A modest energy difference of 0.5 kcal mol^{-1} between the diastereomeric TSs can be attributed to the nearly isosteric *re* and *si* faces with a marginal variation in the differential weak interactions between the catalyst and the reacting partners. Consequently, neither steric nor weak noncovalent interactions are able to impart high *ee* values in the case of **I**.

An instructive comparison between asymmetric sulfoxidation and other known reactions, wherein **I** yielded impressively high *ee* values, is of high significance. In general, the chiral Brønsted acids such as **I** offer bifunctional activation of both electrophilic and nucleophilic reacting partners. In the sulfoxidation reaction, however, the Brønsted acid activates only H$_2$O$_2$, while thioanisole engages in some weak interactions with the catalyst to hold it nearer to the chiral cavity. Because of the absence of sufficient catalyst–substrate interaction, the thioanisole appears to lack an adequate fit in the chiral space provided by the catalyst. Hence, effective transfer of chirality from the chiral Brønsted acid to the substrate fails because of the lack of an organized TS. Furthermore, the geometries of the lowest-energy stereocontrolling TSs in an allyboration and an acetal formation reaction indicated a better fit of the substrate in the chiral pocket of the catalyst.[19] Closer proximity between the chiral elements and the substrate would certainly help induce differential stabilization between the stereocontrolling TSs in such reactions, thus resulting in higher stereoselectivity. However, in the present case, TS **I**-*re*, the substrate thioanisole is positioned away from the chiral cavity provided by the axially chiral catalyst.

After identifying the origin of poor enantioselectivity offered by **I** in the sulfoxidation reaction, we set out to examine the stereocontrolling factors in the case of catalyst **III**. The imidodiphosphoric acids consist of two axially chiral phosphoric acid motifs linked through an imido nitrogen atom. Quite expectedly, the steric environment is very different from the monomeric phosphoric acids hitherto described. It is important to note that **III** offered the best enantioselectivity (98%) in the sulfoxidation of thioanisole.[10]

The closer inspection of the Brønsted acid sites of the catalyst indicates the presence of a confined space for the incoming substrate (Figure 3). As a result of this very feature,
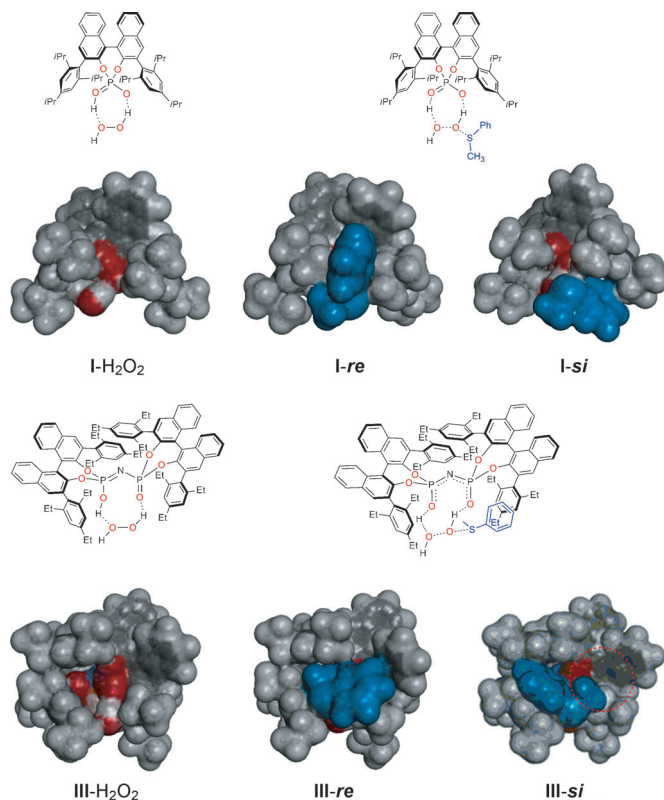

Figure 3. Space-filling models of stereodetermining TSs and the activated H_2O_2 complex with **I** and **III**. The substrate is shown in blue while all carbon atoms of the catalyst are in gray and oxygen atoms are in red. The dotted lines in red show the empty space in **III-si**.

the substrate is expected to experience a severely restricted conformational space, should it dock well on to the catalyst. In fact, we could identify a total of 12 TSs, for both the *re*- and *si*-face additions of the oxygen atom to thioanisole.[14e] The number of possible conformers and the relative dispositions between H_2O_2 and thioanisole is far too limited in the confined space offered by **III** as compared to that for **I**. The incoming thioanisole can approach the preactivated H_2O_2 within the catalyst cavity only in a particular conformation.

The nature of the cavity and the substrate fitting is further understood by using the three-dimensinoal space-filling models. It can be seen that the monomeric catalyst **I** (Figure 3, first row) provides a larger space for the substrate

and hence the guest thioanisole in TSs **I-re** and **I-si** can afford different geometric dispositions with respect to the catalyst/ H_2O_2 host. Even in the lowest energy TS **I-re**, the efficiency of the weak noncovalent interactions responsible for holding the thioanisole in place is found to be low. This situation leads only to a modest energy difference between the *re*- and *si*-face approaches, thus leading to a poor enantioselectivity. Interestingly, in the dimeric catalyst, having a limited space inside the chiral pocket, the substrate appears to find a better fit. A closer perusal of the geometry of the TS **III-re** suggests that the reduced cavity size facilitates an improved interaction between the activated H_2O_2 and the thioanisole, as the latter is forced to remain in the most appropriate conformation for the oxygen-atom transfer. The higher energy diastereomeric TS **III-si** exhibits two key differences. The methyl group of thioanisole does not participate in any favorable interaction with the catalyst and remains slightly away from the activated electrophile as compared to that in the lower energy transition state. The cavity size is found to be relatively larger in TS **III-si**, thus suggesting a kind of induced fit of the substrate when the *si* face has to be exposed to the activated electrophile. Also, the catalyst backbone is found to be relatively more distorted in the higher energy TS **III-si** (see below) Moreover, in TS **III-si**, the fit of the substrate is not ideal as revealed by the empty space shown using the dotted red lines in the figure. In the TS **III-re**, the catalyst and substrate fit perfectly in a lock-and-key fashion. The substrate recognition of this kind is reminiscent of enzymatic reactions wherein the substrates with an optimum size (recognition) and shape (conformation) find improved fit in the enzyme active site.

After probing the gross features such as the size and topology of the cavities in the stereocontrolling TSs, we zoomed in, to examine the finer geometric features. The optimized geometries of the stereocontrolling TSs are provided in Figure 4. The Gibbs free energy of TS **III-re** is 3.9 kcal mol^{-1} lower as compared to that of the diastereomeric TS **III-si** mode of addition. The energy difference of this order is in line with the experimentally observed high enantiomeric excess (98%) obtained using **III**. In an effort to rationalize this vital energy difference, the weak interactions in these TSs are carefully analyzed. It is noticed that in the
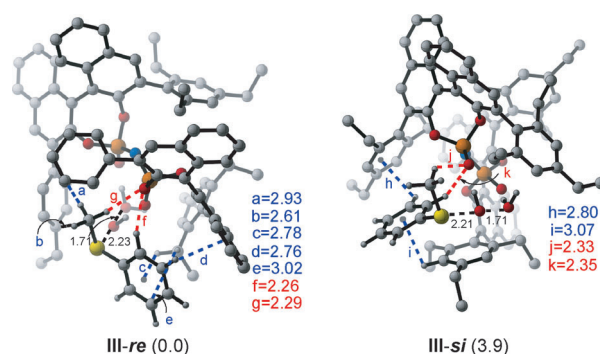

Figure 4. The optimized geometries of the stereodetermining TSs for **III**. The relative free energies (kcal mol^{-1}) are provided in parenthesis. All distances are in Å. The C−H···π, and C−H···O interactions are respectively shown in blue and red.

lower energy TS **III-*re***, the substrate enjoys additional C−H···π and C−H···O interactions. The geometry of the lower energy TS **III-*re*** conveys the presence of a few important stabilizing interactions. Firstly, the aryl ring of the thioanisole engages in three C−H···π (denoted as c, d, and e), as well as one C−H···O interactions (f). Secondly, the CH_3 group of thioanisole participates in two C−H···π (a and b) and one C−H···O (g) interactions with the catalyst. However, in the higher energy TS **III-*si***, the CH_3 group of thioanisole forms only one C−H···O interaction (j). Similarly, the aryl group of thioanisole shows only two weaker C−H···π interactions (h and i). More importantly, the contact distances convey that both these types of interactions (C−H···π and C−H···O) in TS **III-*si*** are weaker as compared to those in TS **III-*re***. The cumulative effect of such differential noncovalent interactions holds the key to the extent of enantioselectivity of this reaction. We have carried out AIM analysis to further verify these interactions. The $\rho_{(bcp)}$ values for C−H···O interactions are found to be within the range of 0.014–0.015 a.u. and that for C−H···π interactions is 0.005–0.01.[20] The roles of C−H···π and C−H···O interactions in asymmetric catalysis have recently been highlighted by other research groups.[21] Since, the stereoselectivity is controlled by such weak interactions, we have also computed the same using the dispersion corrected B3LYP-D3 functional. The calculated *ee* value of greater than 99% is similar to that obtained at the M06-2X level of theory. Although the fit of the right conformer of the substrate to the catalyst cavity appears similar to that in enzymatic processes,[21] the free-energy drive in the present situation is primarily enthalpic and stems from the noncovalent interactions.[22]

Further rationalization of the origin of the differential stabilization in the stereocontrolling TSs is done by using the activation strain analysis. The contribution to the activation energy arising from distortion of the reactants and interaction between the distorted reacting partners is computed.[23] The destabilizing distortion energy of the **III-*si*** is found to be 1.9 kcal mol^{-1} higher than that in the preferred TS **III-*re***. Similarly, the stabilizing interaction in TS **III-*si*** is lower by 2.4 kcal mol^{-1}. The difference in the distortion in the two TSs can be ascertained from the RMSD values of TSs **III-*re*** and **III-*si***, and are 0.015 and 0.024 Å, respectively, with respect to the original catalyst/H_2O_2 complex.[24] These data show that the deviation in TS **III-*re*** is smaller than that in TS **III-*si***.

On the basis of the above-mentioned factors, it appears clear that in the higher energy TS **III-*si*** an induced fit of the substrate leads to a larger cavity size. In other words, when the *si* face is to be exposed to the incoming oxygen atom, the conformation of thioanisole is not as appropriate as that for the *re*-face addition. Furthermore, the best-fit arrangement in the lower energy TS is identified to be governed by the weak noncovalent interactions. In the absence of the well-characterized TSs, as presented in this work, the origin of stereoselectivity would have almost entirely been assigned as arising from steric interactions. These insights could help a) generalize the scope of noncovalent interactions in catalysis, b) in the choice of substrates for sulfoxidation, and c) in the modification of the catalyst backbone for the desired cavity size for a given class of sulphides to find a better fit.

In conclusion, the first TS models for the stereoinduction in imidodiphosphoric acid catalyzed sulfoxidation reaction reveal that the chiral discrimination of the *si* and *re* faces of thioanisole originates from weak C−H···π and C−H···O noncovalent interactions. The fit of thioanisole within the chiral pocket, created by the catalyst/H_2O_2 complex, has been found to be better when the *re* face of the substrate is exposed to the activated electrophile and is reminiscent of enzymatic reactions. The monomeric axially chiral phosphoric acid, having a larger chiral pocket, has been identified to exhibit much weaker interactions between the chiral catalyst and thioanisole, thus leading to larger conformational possibilities for the latter. The computed enantioselectivity has been found to be in very good agreement with the experimental reports for both the monomeric and dimeric catalysts. This study could profoundly simplify the search for TSs for related substrates, as one can start with our lowest energy TS model. The insights on the position and interactions of the substrate with the catalyst could effectively be used in the design of catalyst and substrate variants.

[1] a) *Chiral drugs: Chemistry and biological action* (Eds.: G.-Q. Lin, Q.-D. You, J.-F. Cheng), Wiley, Hoboken, **2011**; b) H. Caner, E. Groner, L. Levy, I. Agranat, *Drug Discovery Today* **2004**, *9*, 105.

[2] a) T. P. Yoon, E. N. Jacobsen, *Science* **2003**, *299*, 1691; b) A. Pfaltz, W. J. Drury III, *Proc. Natl. Acad. Sci. USA* **2004**, *101*, 5723.

[3] S. Caron, R. W. Dugger, S. G. Ruggeri, J. A. Ragan, D. H. Brown Ripin, *Chem. Rev.* **2006**, *106*, 2943.

[4] a) P. Pitchen, E. Duñach, M. N. Deshmukh, H. B. Kagan, *J. Am. Chem. Soc.* **1984**, *106*, 8188; b) F. Di Furia, G. Modena, R. Seraglia, *Synthesis* **1984**, 325; c) E. Wojaczyńska, J. Wojaczyński, *Chem. Rev.* **2010**, *110*, 4303; d) I. Fernández, N. Khiar, *Chem. Rev.* **2003**, *103*, 3651; e) J. Legros, J. R. Dehli, C. Bolm, *Adv. Synth. Catal.* **2005**, *347*, 19; f) H. Srour, P. L. Maux, S. Chevance, G. Simonneaux, *Coord. Chem. Rev.* **2013**, *257*, 3030.

[5] M. Mellah, A. Voituriez, E. Schulz, *Chem. Rev.* **2007**, *107*, 5133.

[6] R. Bentley, *Chem. Soc. Rev.* **2005**, *34*, 609.

[7] a) H. L. Holland, *Chem. Rev.* **1988**, *88*, 473; b) H. L. Holland, *Nat. Prod. Rep.* **2001**, *18*, 171.

[8] a) K. A. Stingl, S. B. Tsogoeva, *Tetrahedron: Asymmetry* **2010**, *21*, 1055; b) F. Shi, M. K. Tse, H. M. Kaiser, M. Beller, *Adv. Synth. Catal.* **2007**, *349*, 2425; c) H. Firouzabadi, N. Iranpoor, A. A. Jafari, E. Riazymontazer, *Adv. Synth. Catal.* **2006**, *348*, 434; d) A. Russo, A. Lattanzi, *Adv. Synth. Catal.* **2009**, *351*, 521.

[9] a) T. Akiyama, J. Itoh, K. Fuchibe, *Adv. Synth. Catal.* **2006**, *348*, 999; b) T. Akiyama, *Chem. Rev.* **2007**, *107*, 5744; c) M. Terada, *Chem. Commun.* **2008**, 4097; d) A. Zamfir, S. Schenker, M. Freund, S. B. Tsogoeva, *Org. Biomol. Chem.* **2010**, *8*, 5262; e) W. Tang, X. Xhang, *Chem. Rev.* **2003**, *103*, 3029; for metal catalysis see: f) R. J. Phipps, G. L. Hamilton, F. D. Toste, *Nat. Chem.* **2012**, *4*, 603; g) M. Mahlau, B. List, *Angew. Chem.* **2013**, *125*, 540; *Angew. Chem. Int. Ed.* **2013**, *52*, 518; h) G. L. Hamilton, E. J.

Kang, M. Mba, F. D. Toste, *Science* **2007**, *317*, 496; i) S. Mukherjee, B. List, *J. Am. Chem. Soc.* **2007**, *129*, 11336; for computational studies see: j) L. Simón, J. M. Goodman, *J. Org. Chem.* **2011**, *76*, 1775; k) L. Simón, J. M. Goodman, *J. Am. Chem. Soc.* **2008**, *130*, 8741; l) T. Marcelli, P. Hammar, F. Himo, *Adv. Synth. Catal.* **2009**, *351*, 525; m) M. Terada, K. Soga, N. Momiyama, *Angew. Chem.* **2008**, *120*, 4190; *Angew. Chem. Int. Ed.* **2008**, *47*, 4122; n) S. Xu, Z. Wang, Y. Li, X. Zhang, H. Wang, K. Ding, *Chem. Eur. J.* **2010**, *16*, 3021.

[10] S. Liao, I. Ćorić, Q. Wang, B. List, *J. Am. Chem. Soc.* **2012**, *134*, 10765.

[11] a) I. Ćorić, B. List, *Nature* **2012**, *483*, 315; b) J. H. Kim, I. Ćorić, S. Vellalath, B. List, *Angew. Chem.* **2013**, *125*, 4570; *Angew. Chem. Int. Ed.* **2013**, *52*, 4474; c) K. Wu, Y.-J. Jiang, Y.-S. Fan, D. Sha, S. Zhang, *Chem. Eur. J.* **2013**, *19*, 474.

[12] a) D. Ajami, J. Rebek, Jr., *Acc. Chem. Res.* **2013**, *46*, 990; b) J. Rebek, Jr., *Acc. Chem. Res.* **2009**, *42*, 1660; c) M. R. Ams, D. Ajami, S. L. Craig, J.-S. Yang, J. Rebek, Jr., *J. Am. Chem. Soc.* **2009**, *131*, 13190; d) R. Breslow, *J. Biol. Chem.* **2009**, *284*, 1337; e) H. Zhao, F. W. Foss, Jr., *J. Am. Chem. Soc.* **2008**, *130*, 12590; f) C. E. Müller, D. Zell, R. Hrdina, R. C. Wende, L. Wanka, S. M. M. Schuler, P. R. Schreiner, *J. Org. Chem.* **2013**, *78*, 8465.

[13] a) C. B. Shinisha, R. B. Sunoj, *J. Am. Chem. Soc.* **2010**, *132*, 12319; b) A. K. Sharma, R. B. Sunoj, *Angew. Chem.* **2010**, *122*, 6517; *Angew. Chem. Int. Ed.* **2010**, *49*, 6373; c) G. Jindal, R. B. Sunoj, *Chem. Eur. J.* **2012**, *18*, 7045; d) All calculations were done using Gaussian09. See the Supporting Information for full details: e) Gaussian09 Revision A.02, Frisch, M. J. et al. Gaussian, Inc, Wallingford, CT, **2004**.

[14] The M06-2X functional has been widely used in literauture to study organocatalytic reactions. See: a) L. Simón, J. M. Goodman, *Org. Biomol. Chem.* **2011**, *9*, 689; b) H. Yang, M. W. Wong, *J. Am. Chem. Soc.* **2013**, *135*, 5808; c) D. A. DiRocco, E. L. Noey, K. N. Houk, T. Rovis, *Angew. Chem.* **2012**, *124*, 2441; *Angew. Chem. Int. Ed.* **2012**, *51*, 2391; d) L. Simón, J. M. Goodman, *J. Am. Chem. Soc.* **2012**, *134*, 16869; e) optimization has been performed for all conformers at the B3LYP level of theory. Further, optimizations have been carried out at the B3LYP-D3 level to account for dispersion effects. See Tables S3,S4 (for **I**) and S7,S8 (for **III**) in the Supporting Information; f) to view the 3D geometries of important TSs, See: http://www.chem.iitb.ac.in/~sunoj/SI_Sulphoxidation/SI_Sulpho.html (Java script required to run). We thank an anonymous referee for suggesting the kinemage tool to generate the 3D images. D. C. Richardson, J. S. Richardson, *Protein Sci.* **1992**, *1*, 3.

[15] A detailed conformational search in which changes in the dihedral angle along the incipient S—O bond, as well as changes in the orientations of the peroxide hydrogen, has been performed. See Figure S1 and Section 1 in the Supporting Information for full details.

[16] a) TS energy computed with respect to the separated reactants, H_2O_2 and thioanisole. b) Sulfoxidation reactions in the absence of catalysts are known to proceed only at higher temperatures (ca. 75 °C). See: M. Jereb, *Green Chem.* **2012**, *14*, 3047.

[17] a) IRC calculations and Wiberg indices clearly show the formation of S—O bond and cleavage of O—O bond take place simultaneously. See Figures S3,S4 and Table S9 of the Supporting Information; b) the BSSE corrected values are provided in the Supporting Information.

[18] A thorough conformational sampling, consisting of as many as 48 unique transition states, is done to identify the most preferred stereocontrolling TSs. See Figure S2 and Tables S1–S4 for in the Supporting Information complete details.

[19] a) M. N. Grayson, S. C. Pellegrinet, J. M. Goodman, *J. Am. Chem. Soc.* **2012**, *134*, 2716; b) I. Ćorić, J. H. Kim, T. Vlaar, M. Patil, W. Thiel, B. List, *Angew. Chem.* **2013**, *125*, 3574; *Angew. Chem. Int. Ed.* **2013**, *52*, 3490; c) Comparison of the optimized geometries of the TSs is given in Figure S5 of the Supporting Information.

[20] a) R. F. Bader, *Atoms in Molecules: A Quantum Theory*, Clarendon, Oxford, **1990**; b) *AIM2000 Version 2.0*; Buro fur Innovative Software, SBK-Software: Bielefeld, Germany, **2002**.

[21] Noncovalent interactions have been invoked to rationalize stereoselectivity in asymmetric organocatalytic reactions. See a) E. H. Krenske, K. N. Houk, *Acc. Chem. Res.* **2013**, *46*, 979; b) R. R. Knowles, E. N. Jacobsen, *Proc. Natl. Acad. Sci. USA* **2010**, *107*, 20678; c) C. Uyeda, E. N. Jacobsen, *J. Am. Chem. Soc.* **2011**, *133*, 5062; d) M. C. Holland, S. Paul, W. B. Schweizer, K. Bergander, C. Mück-Lichtenfeld, S. Lakhdar, H. Mayr, R. Gilmour, *Angew. Chem.* **2013**, *125*, 8125; *Angew. Chem. Int. Ed.* **2013**, *52*, 7967; e) R. C. Johnston, P. H.-Y. Cheong, *Org. Biomol. Chem.* **2013**, *11*, 5057; f) S. E. Allen, J. Mahatthananchai, J. W. Bode, M. C. Kozlowski, *J. Am. Chem. Soc.* **2012**, *134*, 12098; g) see Ref. [14b]; h) P. H.-Y. Cheong, C. Y. Legault, J. M. Um, N. Çelebi-Ölçüm, K. N. Houk, *Chem. Rev.* **2011**, *111*, 5042.

[22] a) The entropic gain obtained through desolvation, as invoked in aqueous enzymatic reactions, is not expected to contribute here; b) we thank the anonymous referee for sharing this insightful view.

[23] See computational methods for a description of the activation strain analysis; a) F. M. Bickelhaupt, *J. Comput. Chem.* **1999**, *20*, 114; b) A. Diefenbach, F. M. Bickelhaupt, *J. Phys. Chem. A* **2004**, *108*, 8460; c) C. Y. Legault, Y. Garcia, C. A. Merlic, K. N. Houk, *J. Am. Chem. Soc.* **2007**, *129*, 12664.

[24] a) The PyMOL Molecular Graphics System, Version 1.2r3pre, Schrödinger, LLC; b) the increased distortion in TS **III-si**, as noted through the root mean square deviation (RMSD) values, can also be understood by comparing some pertinent geometric parameters as illustrated in Figure S6.